JOURNAL OF MATERIALS SCIENCE 33 (1998) 1653–1660

# Elevated temperature mechanical properties of $MoSi_2/Si_3N_4$, $MoSi_2/SiC$ composites produced by self-propagating high temperature synthesis

A. H. BARTLETT*, R. G. CASTRO
*Los Alamos National Laboratory, Los Alamos, NM 87545, USA*

$MoSi_2/Si_3N_4$ and $MoSi_2/SiC$ composite powders were produced via a novel self-propagating high temperature synthesis technique (SHS) and consolidated both by hot-pressing and plasma spraying. Mechanical testing subsequently was performed under four-point bending at a variety of elevated temperatures and strain rates. Damage accumulation in the hot-pressed materials, either by particle cracking or particle/matrix separation, resulted in composite mechanical properties that were reduced below the level of the unreinforced material. Plasma sprayed materials showed power-law hardening behaviour caused by $Mo_5Si_3$ precipitates and increased strain tolerance because of the fine grain size and reduced yield strength of the matrix. © *1998 Chapman & Hall*

## 1. Introduction

Molybdenum disilicide is a candidate high temperature structural material owing to its excellent oxidation resistance, stability with reinforcing phases, and a ductile to brittle transition temperature at around 1100 °C which gives it high toughness at elevated temperatures. The major limitations associated with its high temperature use are a reduction of strength, and creep. It is well known that hard reinforcing phases can give both strength and creep resistance benefits to ductile matrices; these benefits sensitively depend upon reinforcement volume fraction, reinforcement geometry, and high temperature properties of the matrix itself [1, 2]. Previous research has investigated the effects of various whisker, platelet, and fibre reinforcements on the mechanical response, in particular the creep resistance, of $MoSi_2$, e.g. [3, 4]. Up to now, reinforcements have been introduced primarily by mechanical mixing or *in situ* synthesis; moreover, the great majority of mechanical strength data has come from samples tested in compression. Disadvantages in the processing techniques lie in the unequal distribution of the reinforcing phase and, more importantly, in the size limits of the reinforcing phase. (Rösler *et al.* [5] have shown that creep resistance, and by extension any dislocation–motion limited power law behaviour, improves with decreasing size of the hardening phase, such that optimum behaviour is obtained at the smallest particle size for a given volume fraction.) The major drawback of strength testing in compression is that damage development, which is a critical limit to strength of composite materials, is suppressed or, when observed, is of a different nature than that seen under tension.

In this work, $MoSi_2/Si_3N_4$ and $MoSi_2/SiC$ composite powders were produced via a novel self-propagating high temperature synthesis technique (SHS). The advantages in the SHS process lie in its low cost, and, with high temperature deformation as a consideration, in the ability to form powders with very fine second phase particles. The bulk of this paper will discuss the stress–strain response of composites made from SHS powders, consolidated both by hot-pressing and plasma spraying, and subsequently tested under four-point bending at a variety of temperatures and strain rates. Microstructural characterization, by scanning electron microscopy (SEM) and X-ray diffraction, will be used to understand the observed behaviours, and comparison with existing models for ductile matrix composites will be made. The development of damage during testing will be characterized, and its limiting role in strength development will be highlighted.

## 2. Experimental procedure

Generalities of the SHS process are discussed elsewhere [6, 7]. In the case of nitride formation, such as $Si_3N_4$, the SHS process is usually carried out in a reactor pressurized with nitrogen. The gas infiltrates the porous reactant mixture, reaches the combustion front and reacts with the precursors to form the desired nitrides. The SHS process produces low density sponges which are further processed by crushing and milling to produce powders. In another paper [8], the powders were characterized by transmission electron microscopy (TEM) which revealed that the reinforcing phase, both for SiC and $Si_3N_4$, occurred as small,

*Current address: Norsam Technologies, 61 Rover Blvd, Los Alamos, NM 87544, USA.

TABLE I Hot-pressing parameters

| | |
|---|---|
| Powder | $MoSi_2$ (30 g) |
| Die diameter | 3 cm |
| Pre-press temperature/time | 1200 °C/5 min |
| Pre-press pressure | 1.952 MPa |
| Hot-press temperature/time | 1800 °C/5 min |
| Hot-press pressure | 1.952 MPa |
| Atmosphere | Ar |

TABLE II Plasma spraying parameters

| | |
|---|---|
| Torch | SG-100 Plasmadyne |
| Amps | 1000 |
| Volts | 32.5 |
| Primary arc gas | Ar 25 slm[a] |
| Secondary arc gas | He 15 slm |
| Powder carrier gas | Ar 8 slm |
| Powder feed rate ($g\,min^{-1}$) | 7.56 |
| Atmosphere | Ar 66.5 kPa |
| Spray distance | 87 mm |
| Anode/Cathode | 730/129 |

[a]slm, standard litres per minute.

< 50 nm particles distributed around the surface of the $MoSi_2$ powder. These powders were then consolidated into discs by hot-pressing under the conditions listed in Table I.

Samples were also produced from the SHS powders via plasma spray processing, under the conditions listed in Table II. Thick deposits of sprayed materials were built up by translating the torch over a graphite substrate (Poco™ AXM-5Q); a bell shaped deposit was built up from which samples large enough for mechanical testing were obtained. Only the $MoSi_2/Si_3N_4$ composite material was able to be sprayed for testing, however. Gross cracking of the $MoSi_2$/SiC deposits precluded obtaining pieces for mechanical testing, and as such will not be discussed further.

Mechanical testing of the hot pressed powders was carried out at 1200, 1300 and 1400 °C in air, at cross-head rates of $4.0\,\mu m\,s^{-1}$ and $0.4\,\mu m\,s^{-1}$. The strain rate depended on the geometry of each piece, but corresponded to $\approx 10^{-4}\,s^{-1}$ and $10^{-5}\,s^{-1}$ respectively. Test beams were cut to nominal dimensions 2.5 × 2.5 × 25 mm and tested in a high temperature SiC four-point semi-articulating fixture. Loading was applied parallel to the direction in which the samples were hot-pressed. For comparison, hot pressed samples of monolithic $MoSi_2$ were also tested under the same conditions.

The plasma-sprayed $MoSi_2/Si_3N_4$ samples were tested only at 1200 °C, at a strain rate of $\approx 10^{-5}\,s^{-1}$. For comparison, a sprayed sample of monolithic $MoSi_2$, sprayed under the same conditions, was also tested.

## 3. Results and discussion

Stress–strain curves for all of the hot-pressed samples are shown in Fig. 1a–d. The strain data were taken directly from the set cross-head speed and were not able to be corrected for machine compliance, resulting in overestimates of strain by a factor of approximately 3 in the rising portion of the curves. The plastic strain in the flatter portions of the curves will not be significantly affected by the lack of compliance calibration. Stress values were calculated assuming linear-elastic response, which in this case resulted in an overestimate of true stress by up to 20% in the non-linear portion of the curves. This can be corrected for by standard techniques (if the strain values are first corrected) [9].

General trends were evident in all testing conditions, most obvious that yield stress and ultimate strength decreased and strain to failure increased with increasing testing temperature and decreasing strain rate. The strain rate and temperature dependence of yield strength in monolithic $MoSi_2$ has been well documented [10, 11], and is a function of temperature dependence and strain rate sensitivity of the active slip systems. Matrix-controlled composite yielding followed the same trends as the monoliths, as has been observed in other reinforced systems, e.g. Al–SiC [12]; however, this trend is not necessarily expected, as yield strength can be very sensitive to microstructure and sample history [2]. Ultimate strength and strain to failure are controlled by damage accumulation in the composite, and will be discussed in detail below.

The hot-pressed $MoSi_2/Si_3N_4$ composites exhibited a consistently higher yield strength than the hot-pressed $MoSi_2$/SiC. Volume fractions of the reinforcing phase in the $MoSi_2$/SiC composites, as determined by image analysis, were 20–30 vol% SiC, while the $MoSi_2/Si_3N_4$ had a vol% $Si_3N_4$ of 10–20%, pointing out that the amount of the hard phase is not the only factor in determining yield strength. It is not possible to ascribe this difference to any one aspect of the composite microstructure. Yield behaviour of a reinforced composite is known to be sensitive to (at least) reinforcement morphology, its distribution in the matrix, its volume fraction, and matrix yield strength [1, 2, 13]. In this case, the $Si_3N_4$-reinforced matrix has a much larger grain size. It has been shown that grain size has a strong effect on the yield behaviour of $MoSi_2$ [14], and would then be expected to influence composite yield strength. The dramatic difference in reinforcement distribution (Fig. 2a, b) will also strongly affect composite yield behaviour in a fashion that cannot be predicted *a priori*. More careful experimentation would be required to sort out all contributing influences.

Hot-pressing of the $MoSi_2$/SiC powders led to nearly complete densification of the silicide phase, and significant agglomeration of the SiC, resulting in SiC particle sizes of up to 20 μm (Fig. 2a). These large agglomerates were evenly distributed throughout the matrix and located on $MoSi_2$ grain boundaries. After testing, in all samples, multiple numbers of large cracks initiated at the tensile surface and propagated stably through the sample. Damage-zone evolution ahead of these major crack tips, at all testing temperatures and strain rates, occurred by cracking within the SiC agglomerates. Neither matrix failure nor interface decohesion was observed. Fig. 3 is the 1400 °C, $10^{-5}\,s^{-1}$ sample, showing incipient cracking of the SiC occurring ahead of one of many cracks that were

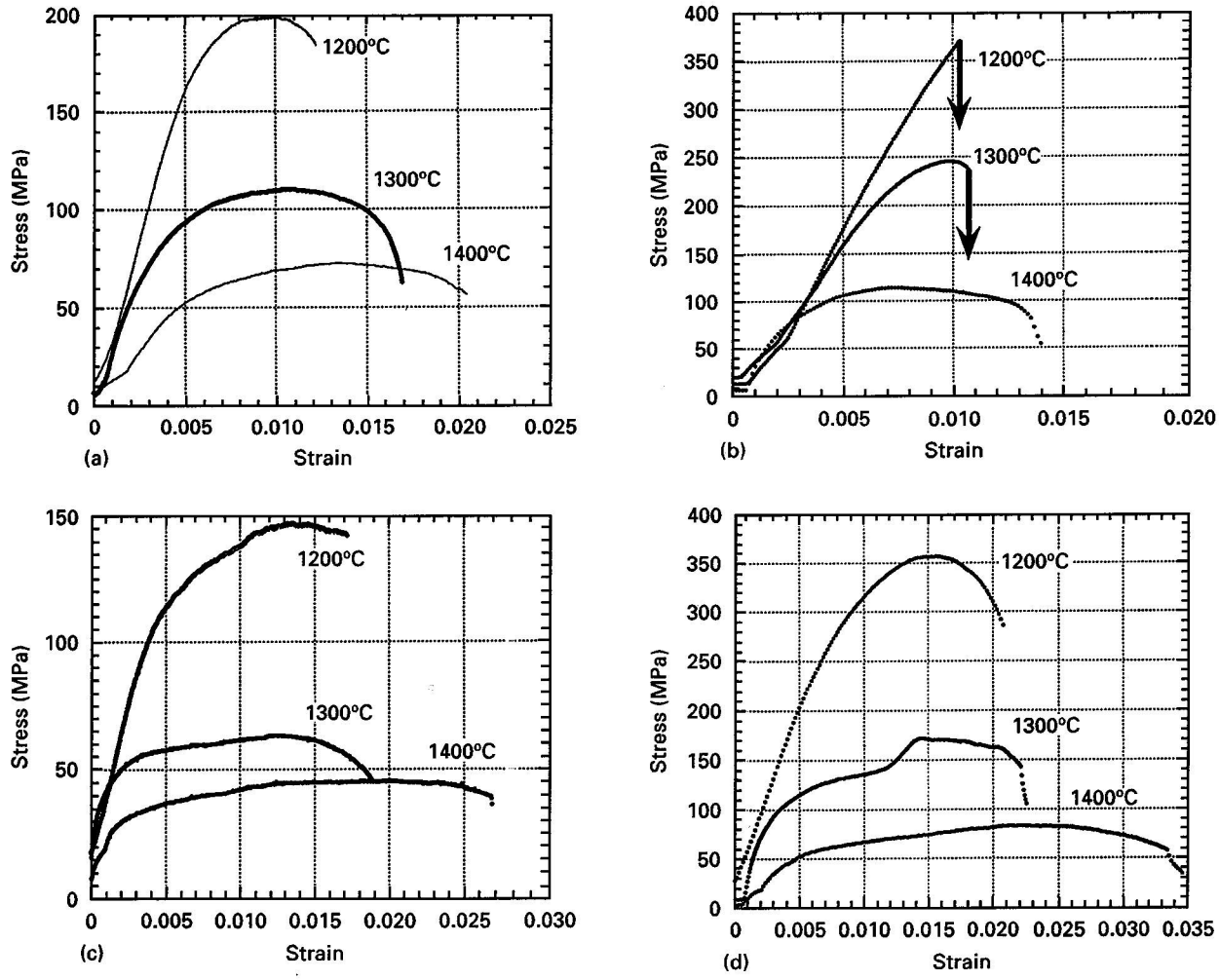


*Figure 1* Stress–strain curves for hot-pressed samples at all temperatures and strain rates. (a, c) $10^{-5}\,s^{-1}$; (b, d) $10^{-4}\,s^{-1}$. (a, b) $MoSi_2/Si_3N_4$; (c, d) $MoSi_2/SiC$.

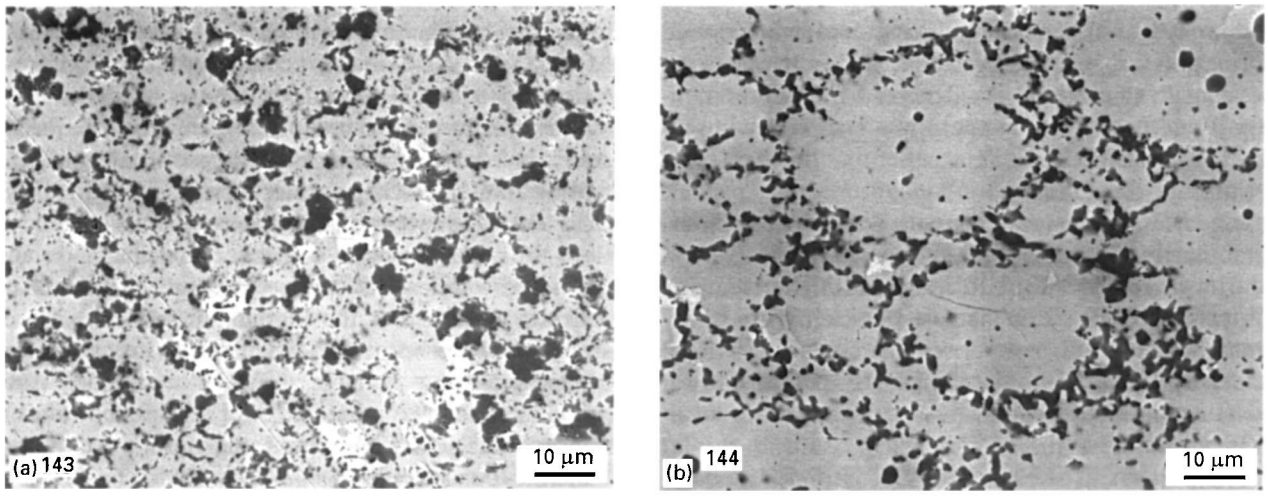


*Figure 2* (a) Microstructure of hot-pressed $MoSi_2/SiC$. Dark phase is SiC. (b) Microstructure of hot-pressed $MoSi_2/Si_3N_4$. Dark phase is $Si_3N_4$.

present in the sample. The higher temperature samples exhibited a damage zone around the major cracks that was more widespread than that observed in the lower temperature samples. The lower temperature samples had fewer major cracks, in part because they failed at strain values that were approximately half of the higher temperature samples. However, differences in testing temperature or strain rate did not change the type of damage that occurred, only the extent of it.

The $MoSi_2/Si_3N_4$ powders showed even more pronounced agglomeration of the $Si_3N_4$ after hot pressing; Fig. 2b shows that these agglomerates were located almost exclusively on the $MoSi_2$ particle boundaries. (Interestingly, nearly complete densification of these $Si_3N_4$ agglomerates occurred despite the absence of any intentional sintering aids.) Damage in these composites was similar to the $MoSi_2/SiC$ composites; all samples had multiple major cracks, with

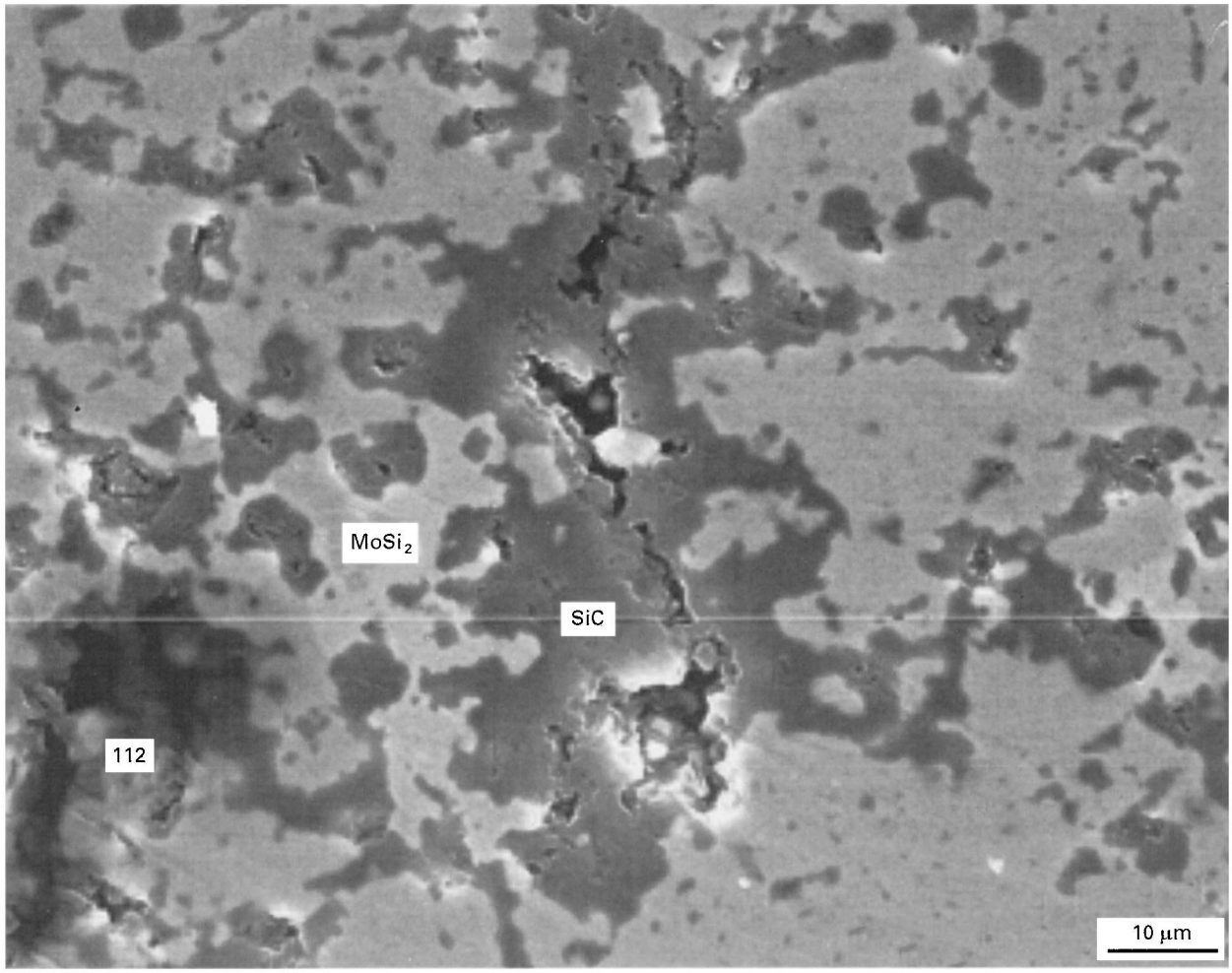


*Figure 3* Cracked SiC particles in hot-pressed $MoSi_2$/SiC tested at 1400 °C and $10^{-5}\,s^{-1}$.

damage zones ahead of these crack tips. They differed in that damage occurred by $MoSi_2/Si_3N_4$ interface failure (Fig. 4). Particle cracking and matrix void formation was not observed. The higher temperature tests again showed more widespread and diffuse damage than the lower temperature samples, with no change in the mode of damage. Because the $Si_3N_4$ was primarily on grain boundaries or prior particle boundaries, the major crack path was primarily intergranular/interparticle (Fig. 5).

The increased strain tolerance at higher temperatures is a result of the increased crack growth resistance of the $MoSi_2$ matrix with temperature. At the same applied strain, the higher temperature/lower yield strength composite will experience greater localized strain near the reinforcing phase and similar levels of triaxial stresses between particles as compared to the lower temperature/higher yield strength composites [2]. This combines with the greater crack growth resistance of the matrix to give larger damage zones ahead of major cracks. The damage both absorbs strain energy and reduces the effective stress intensity at the major crack tip by microcracking-type processes [15]. Multiple cracking, particularly pronounced in the higher temperature samples, also reduces the effective applied stress intensity at major crack tips [16] and promotes greater strain tolerance. These effects result in more stable major cracks, indicated by their increased strain to failure.

Despite their damage tolerance, composite mechanical behaviour does not compare favorably to monolithic $MoSi_2$. Fig. 6 shows the stress–strain response of $MoSi_2/Si_3N_4$ SHS powders compared with unreinforced hot-pressed $MoSi_2$; the ultimate strengths and strains to failure of the composites are greatly reduced compared to the monolith. Any potential gains in adding reinforcements are apparently discounted by early damage developing in the composite. In addition, the yield strengths of the composite materials decreased with respect to the unreinforced matrix. In order to ensure that the initial non-linearity of the stress–strain curves of the SHS material was caused by plasticity and not damage, some of the samples were unloaded and then reloaded, after an initial strain of approximately 0.15% beyond the onset of non-linearity. Upon reloading there was no observable change in modulus, nor was damage detected by high resolution SEM. The drop in the yield point of the reinforced samples therefore can be considered a true plasticity phenomenon, and can be rationalized by other work that has detailed the role of prestressing and second phases on the yield strength of $MoSi_2$. Dislocations will be generated in the matrix upon cool-down from processing conditions because of coefficient of thermal expansion mismatch between the matrix and reinforcement. The effect of higher dislocation densities prior to testing has been shown to result in plastic deformation of $MoSi_2$ at lower temperatures

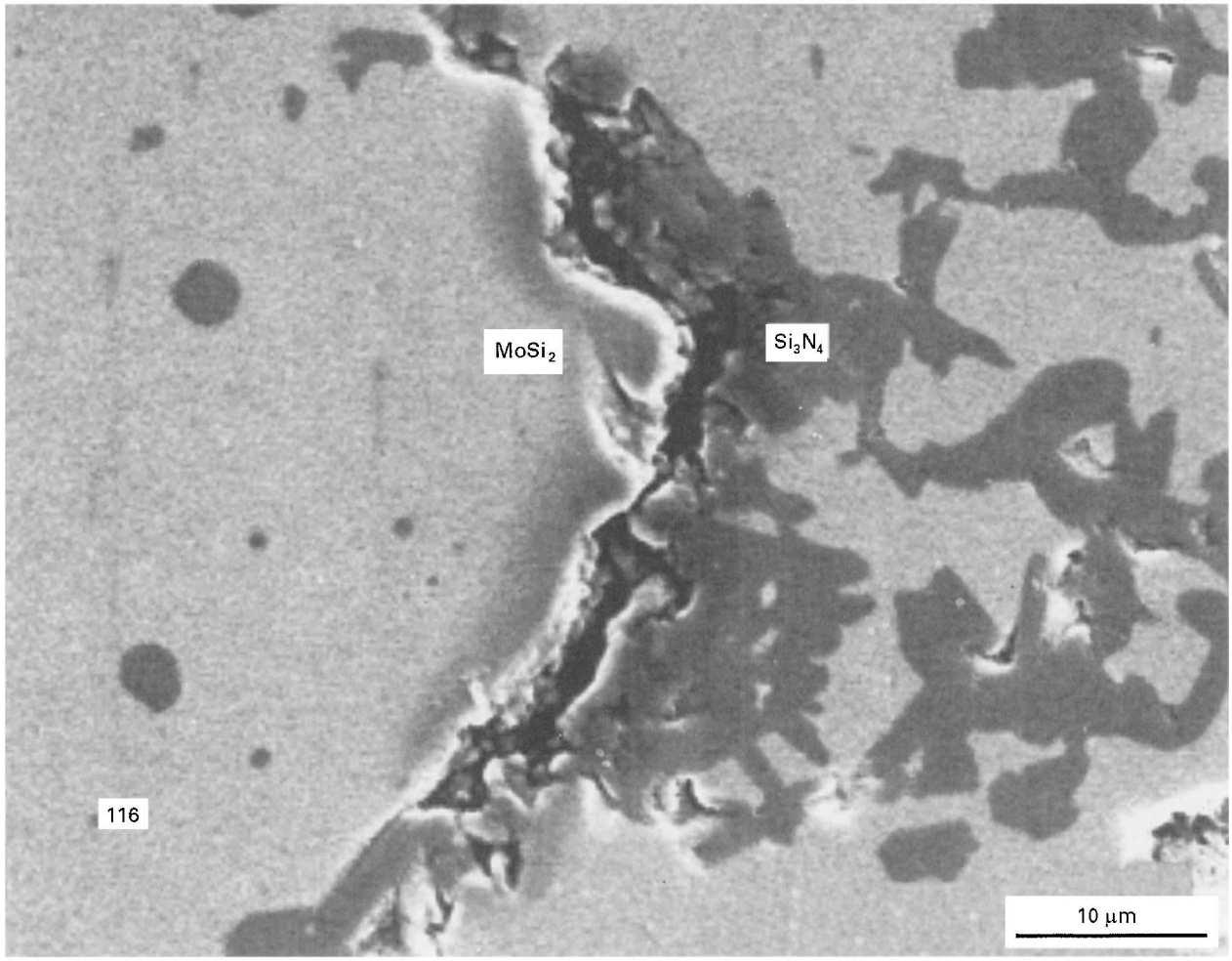


*Figure 4* Interfacial separation in the $MoSi_2/Si_3N_4$ hot-pressed powders, tested at 1400 °C and $10^{-5}\,s^{-1}$.

and stresses [17]. Moreover, second phase interface and grain boundaries have been shown to serve as efficient dislocation sources in $MoSi_2$ composites [18]. While these effects would be expected to reduce matrix yield strength, it should also be noted that in any ductile matrix the presence of hard reinforcements will lead to localized yielding at applied global stress levels much lower than the nominal yield strength of the matrix. This localized yielding, if affecting a large enough volume, can result in a reduced composite yield stress, as has been seen, for example, in the Al/SiC system, especially at lower reinforcement volume fractions [13].

The plasma-sprayed material showed lower yield strengths and ultimate strengths compared to the hot-pressed materials, but exhibited power-law hardening behaviour and a much greater strain tolerance. The stress–strain curves of the monolithic $MoSi_2$ and SHS $MoSi_2/Si_3N_4$ plasma sprayed materials, tested at 1200 °C and $10^{-5}\,s^{-1}$ are given in Fig. 7. The SHS sprayed material showed higher yield strength than the sprayed monolith; the power law behaviour indicates hardening behaviour without significant damage development. TEM and X-ray diffraction revealed that little of the $Si_3N_4$ was retained during spraying of the SHS powder [8], while substantial amounts of $Mo_5Si_3$ were found in the matrix. Because $Mo_5Si_3$ is linearly elastic at these temperatures [19], the increase in mechanical properties of the sprayed SHS powders can be attributed to the trisilicide acting as a reinforcing phase. A backscattered micrograph of the sprayed SHS material is shown in Fig. 8; the darker phase in $MoSi_2$, and the lighter is $Mo_5Si_3$, with in-between shadings representing a eutectic mixture. Image analysis suggests a volume fraction of $Mo_5Si_3$ of 25–50%. The stress–strain curve of the SHS sample was analysed using the finite element method (FEM) analysis of Bao *et al.* [1], which assumes continuum behaviour of the matrix material in modelling the effects of a hard second phase (Fig. 7). Using the stress–strain curve of the unreinforced $MoSi_2$ to model matrix response (noting that minimal $Mo_5Si_3$ was found in the unreinforced deposit), and assuming spherical, equally distributed particles of $Mo_5Si_3$ (a lower bound estimate), the model predicts that the hardening experienced by the sample is caused by a reinforcement volume fraction of 40%, consistent with the $Mo_5Si_3$ volume fraction. $Mo_5Si_3$ has been previously investigated as a thermodynamically stable reinforcing phase whose efficacy sensitively depends upon grain size and reinforcement morphology. Its effectiveness in this system as compared to other work [19] probably results from the absence of dynamic grain refinement during testing. The very fine grain size is also

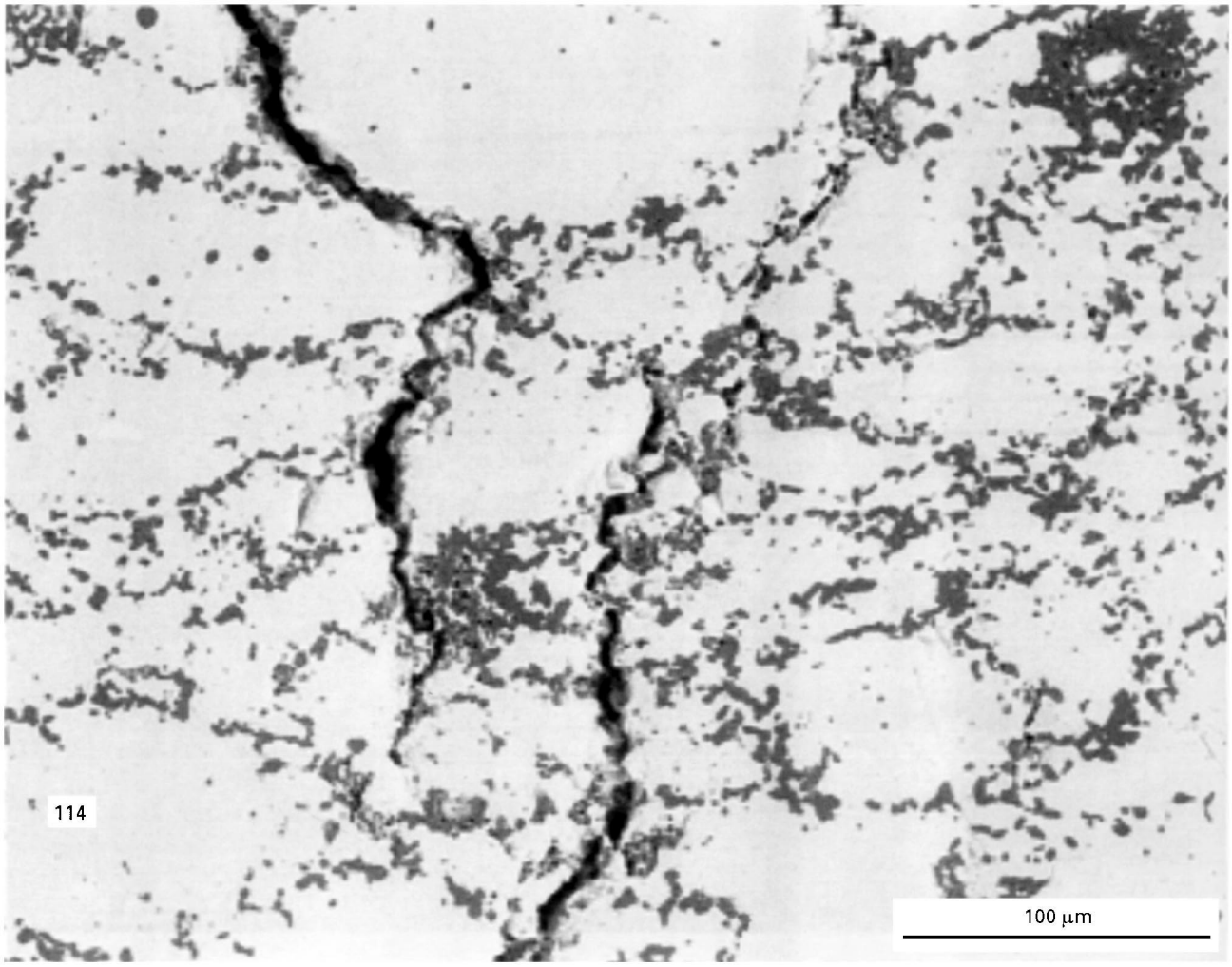


*Figure 5* Gross cracking behaviour in the $MoSi_2/Si_3N_4$ hot-pressed powders, tested at 1400 °C and $10^{-5}\,s^{-1}$.

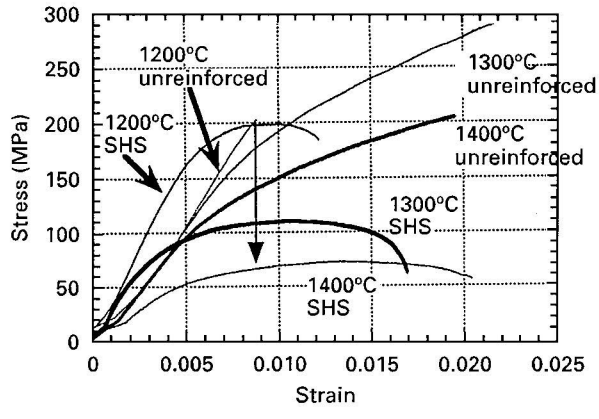


*Figure 6* Comparison of the stress–strain response of hot-pressed SHS $MoSi_2/Si_3N_4$ with monolithic hot-pressed $MoSi_2$, at $10^{-4}\,s^{-1}$

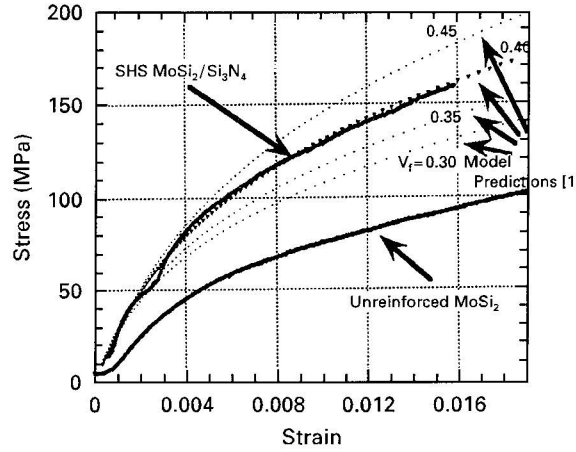


*Figure 7* Stress–strain curves of plasma-sprayed SHS $MoSi_2/Si_3N_4$ powders and monolithic sprayed $MoSi_2$, at 1200 °C and $10^{-5}\,s^{-1}$. FEM analysis of Bao *et al.* [1] is shown for comparison, at various volume fractions of reinforcing phase.

responsible for the much reduced stress levels that plasma sprayed materials are capable of sustaining as compared to hot-pressed materials [20].

The modestly large strains experienced by the SHS sprayed materials can be explained by their relatively low yield strengths, which in turn are a consequence of fine grain size. Damage, either in the form of particle cracking or interface decohesion, limits the amount of strain the composite can sustain, and it in turn is directly affected by the stress sustained at or in the vicinity of the particle. Sufficiently low yield strength matrices flow at stresses prior to damage accumulation and therefore prevent damage from initiating. This trend has clearly been seen in other work, e.g. [12] which showed that damage in Al/SiC composites

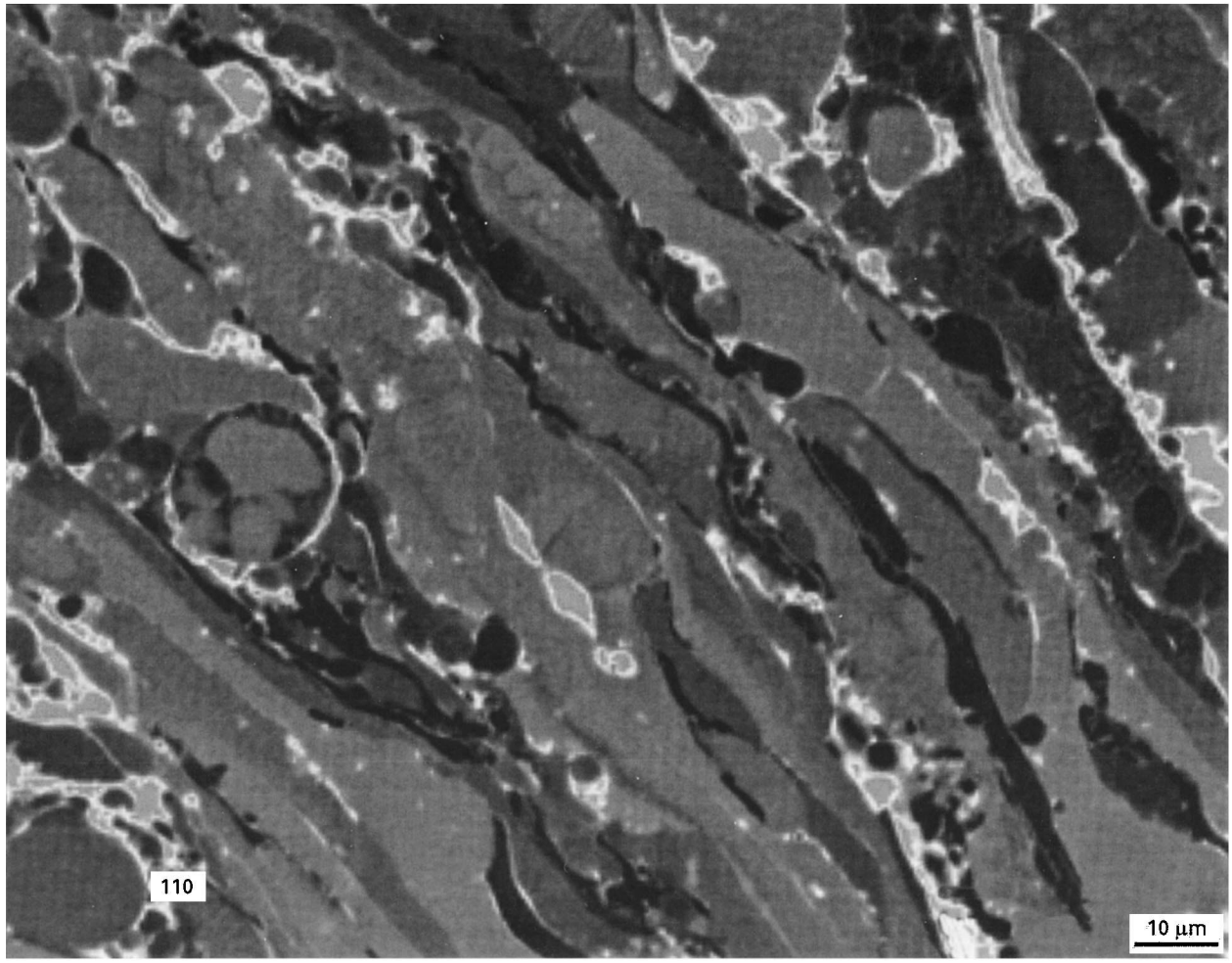


*Figure 8* Backscattered SEM image of plasma sprayed $MoSi_2/0.50\ Si_3N_4$. The dark phase is $MoSi_2$, the light is $Mo_5Si_3$, and in-between shadings are the eutectic.

was suppressed with lower yield strength matrices. It is not known which combinations of matrix flow stress, interface and particle strengths, strain, and reinforcement volume fraction are necessary to entirely prevent damage.

## 4. Concluding remarks

The use of SHS to produce $MoSi_2/SiC$ and $MoSi_2/Si_3N_4$ composite powders has been shown to be an economical method of producing powders of desirable morphology. The most significant problem with these powders is agglomeration of the initially fine-sized reinforcements during hot pressing, which leads to mechanical properties of the composite that are less than ideal. Cracking of the SiC agglomerates and interface separation in the $MoSi_2/Si_3N_4$ composites during testing is not surprising because of their large size. It is well documented that this type of damage could be suppressed if a finer particle size were incorporated [21]. Further post-processing of the SHS powders, e.g. more carefully controlled milling to more homogeneously distribute the reinforcing phase, may achieve this result. It appears that one of the microstructural requirements to minimize damage accumulation, that is, a reduction in reinforcement particle size, complements the requirements for increased strength and creep resistance. On the other hand, the large strains experienced by the plasma sprayed materials suggest that a finer $MoSi_2$ grain size could also result in greater strain tolerance by allowing for better accommodation during deformation. This would occur, though, at the cost of lower yield strengths and decreased creep resistance; microstructure optimization might require a balance between strength and damage tolerance.

One final benefit of incorporating $Si_3N_4$ is that it has been shown to nearly eliminate pest oxidation when arranged in the matrix properly [22]. It is not known if microstructure design for pest minimization coincides with that which optimizes mechanical properties. As well, matrix/reinforcement decohesion observed during testing indicates a relatively weak interface, which will have important effects on global mechanical response. The chemistry and mechanical behaviour of this interface needs to be further addressed.

## References

1. G. BAO, J. W. HUTCHINSON and R. M. McMEEKING, *Acta Metall. Mater.* **39** (1991) 1871.

2. T. CHRISTMAN, A. NEEDLEMAN and S. SURESH, *Acta Metall.* **37** (1989) 3029.
3. R. M. AIKIN, *Mater. Sci. Eng.* **A155** (1992) 121.
4. F. D. GAC and J. J. PETROVIC, *J. Amer. Ceram. Soc.* **68** (1985) C200.
5. J. RÖSLER and E. ARZT, *Acta Metall. Mater.* **38** (1990) 671.
6. R. KNIGHT, R. W. SMITH and M. MOHANTY, *Proceedings 8th National Thermal Spray Conference*, ASM International, Materials Park, OH, edited by C. C. Berndt and S. Sampath (1995) p. 743.
7. Z. A. MUNIR and V. ANSELMI-TAMBURINIA, *Mater. Sci. Rep.* **3** (1989) 277.
8. H. KUNG, Y. LU and A. H. BARTLETT, *J. Mater. Res.* in press.
9. A. NADAI, *Theory of flow and fracture of solids* (McGraw-Hill, New York, 1950) p. 353.
10. S. A. MALOY, T. E. MITCHELL, J. J. PETROVIC, A. H. HEUER and J. J. LEWANDOWSKI, *Mater. Res. Soc. Proc.* **322** (1994) 21.
11. R. GIBALA, A. K. GHOSH, D. C. VAN AKEN, D. J. SROLOVITZ, A. BASU, H. CHANG, D. P. MANSON and W. YANG, *Mater. Sci. Eng. A* **A155** (1992) 147.
12. S. F. CORBIN and D. S. WILKINSON, *Acta Metall. Mater.* **42** (1994) 1329.
13. A. LEVY and J. M. PAPAZIAN, *Met. Trans. A* **21A** (1989) 411.
14. A. K. GHOSH and A. BASU, *Mat. Res. Soc. Proc.* **322** (1994) 215.
15. J. W. HUTCHINSON, *Acta Metall.* **35** (1987) 1605.
16. H. M. SHU, J. PETIT and G. BEZINE, *Engng Fract. Mech.* **94** (1994) 933.
17. H. CHANG and R. GIBALA, *Mater. Res. Soc. Symp. Proc.* **322** (1994) 223.
18. R. GIBALA, H. CHANG and C. M. CZARNIK, *ibid.* **322** (1994) 175.
19. D. P. MASON and D. C. VAN AKEN, *Acta Metall. Mater.* **43** (1995) 1201.
20. R. GIBALA, A. K. GHOSH, D. C. VAN AKEN, D. J. SROLOVITZ, A. BASU, H. CHANG, D. P. MASON and Y. YANG, *Mater. Sci. Eng.* **A155** (1992) 147.
21. J. YANG, C. CADY, M. S. HU, F. ZOK, R. MEHRABIAN and A. G. EVANS, *Acta Metall. Mater.* **38** (1990) 2613.
22. M. G. HEBSUR, *Mater. Res. Soc. Symp. Proc.* **350** (1994) 177.

*Received 19 April 1996*
*and accepted 22 May 1997*